Identification of Targetable Surfaces of Cks1 for Development of New Cancer Therapeutics

Nolan M. Winicki[1], Reed E. S. Harrison[1], J. Jefferson P. Perry[2], Dimitrios Morikis[1]

1 Department of Bioengineering

2 Department of Biochemistry

ABSTRACT

Cyclin-dependent protein kinase regulatory subunit 1 (Cks1) is involved in cell cycle progression through interactions with cyclin-dependent kinases (CDK) and ubiquitination of cyclin-dependent kinase inhibitors (CKI). Dysfunction of CDK dependent associations can affect the entrance of a cell into mitosis, particularly the G1-S phase transition. Abnormal assistance from Cks1 with the multiprotein complex SCF (Skp2) in the ubiquitination of CDKN1B ($p27^{Kip1}$) can disrupt the mitotic regulatory protein levels escalating to cancer development. In this study, we use computational methods to investigate interactions in three different complexes sharing Cks1 in order to create a targeted pharmaceutical solution that will assist in regulation. Our analysis is performed using the crystal structure of Cks1 in three complexes to include involvement between one ubiquitin ligase and two CDKs. The assessment is based on the intermolecular electrostatic interactions, such as hydrogen bonds and charge-charge interactions. We observe that charge and hydrogen bonding plays a significant role in the stability between Cks1 and adjacent proteins in each complex. Due to large binding interfaces and varied distribution of charge across the main contact regions, we decided that a condensed pocket on Cks1 that interacts with phosphorylated $p27^{Kip1}$ should be selected for further in-depth examination.

Nolan Winicki

Department of Bioengineering

Nolan Winicki is a third-year Bioengineering major. Nolan has been doing research in the Biomolecular Modeling and Design Lab under the guidance of Dr. Dimitrios Morikis since his sophomore year. He studies mitotic regulatory proteins for the creation of targeted cancer therapeutics and is currently a member of the Student Editorial Board for the University of California, Riverside Undergraduate Research Journal. Nolan plans to pursue a career in medicine.

FACULTY MENTOR

Dr. Dimitrios Morikis

Professor in the Department of Bioengineering

Professor Morikis' work focuses on immune system function and regulation, structure-dynamics-interactions-activity/function relations, design of peptides and proteins with tailored properties, drug and biomarker discovery, development of structural and translational bioinformatics methods, and systems immunology and disease modeling. His research is predominantly computational, with emphasis on molecular dynamics simulations, electrostatic calculations, free energy calculations, pharmacophore modeling, virtual screening, and protein-ligand docking, and has an experimental component, with emphasis on binding, biochemical, and functional assays and NMR spectroscopy. Nolan's work includes graduate student Reed Harrison, and is a collaborative project with Professor Jefferson Perry of UCR's Department of Biochemistry.

INTRODUCTION

During interphase of the cell cycle in eukaryotes, the G_1, S, and G_2 phases occur sequentially, and during the transition from G_1 to S there is a checkpoint to determine whether or not the cell will replicate cellular DNA. Once crossed, the cell will divide into two daughter cells and carry out normal cell processes until the next G1 phase without interruption. Cyclin Dependent Kinases (CDK) form complexes with cyclins during short periods of the cell cycle to regulate steps of progression. Specifically, cyclin-dependent protein kinase regulatory subunit 1 (Cks1) binds to a catalytic subunit, a cyclin-dependent kinase. Regulation of the cell cycle depends on the interactions between cyclins, CDKs, and CDK inhibitors (CKIs). Dysregulation of the cell cycle results in uncontrolled, damaged cell multiplication that may lead to cancerous growths.

While the concentration of mitotic regulatory proteins oscillates during stages of the cell cycle due to periodic proteolysis, the ubiquitin-proteasome system maintains the levels of degradation.[6] This system involves multiple enzymes and a ubiquitin ligase which dictates the specificity of ubiquitination. One of the ligases is the S-phase kinase-associated protein 2 (Skp2) which is part of the SCFSkp2 complex. This complex targets cell cycle control elements, primarily p27 and p21, tagging them for destruction.[4,5] Cyclin-dependent kinase inhibitor 1B ($p27^{Kip1}$) is incredibly influential on cell cycle division due to binding and preventing the activation of E-CDK2 during the G1 phase.[3] While levels of $p27^{Kip1}$ fluctuate with the cell cycle, modulation is done by the SCF-Skp2 complex creating an inverse relationship of concentrations.[4] While normal levels regulate cell cycle progression, a recent study showed that overexpression of Skp2 is frequently observed in human cancer progression.[2] In addition, Skp2 inactivation restricts cancer development when observed in oncogenic conditions in vivo.[1] Cks1 plays a critical role in $p27^{Kip1}$ ubiquitination by increasing the binding affinity of Skp2 for $p27^{Kip1}$.

Using structural analyses of protein complexes that focus on hydrogen bonds and electrostatic interactions, this project will search for the amino acid interactions between proteins that contribute the largest amount of stability to the protein complex. Determining key interactions can help design new drugs to alter protein-protein interactions. These drugs have potential applications as new cancer therapeutics, acting by restoring regulation of cell cycle progress and slowing the growth rate of tumors. Additionally, the shape of protein-protein interfaces are considered to account for druggability of protein-protein interactions. After determining the most promising interactions, molecular dynamics simulations will be performed for fine-grain analysis leading to identification of key amino acid interactions that a new therapeutic should disrupt.

METHODS

Structure Retrieval and Preparation

The crystallographic structures for protein complexes Skp1-Ckp2-Cks1-$p27^{Kip1}$, CDK1-Cks1, CDK2-Cks1 were retrieved from the Protein Databank (PDB) with identifiers 2AST, 4YC6, and 1BUH, respectively, and were visualized using the software UCSF Chimera.[11] The initial structures were missing hydrogens and heavy atoms in addition to a chimeric region on Skp2 which however was not involved in the binding interface. These discrepancies were remedied through the tools PDBFixer and Modeller, and the hydrogens were assigned based at pH 7.4.

Structural Analysis of Hydrogen Bonding

Four separate analyses were performed to characterize the structural and electrostatic components of interactions in the protein complexes. The first test was to search for hydrogen donor-acceptor pairs to determine potential attractive dipole-dipole interactions that could add to the stability of the complex. This was done by quantitatively measuring the amount of hydrogen bonds and the distance between each heavy atoms. The default hydrogen bond constraints in UCSF Chimera[10] with relaxations of 0.4 Å and 30° were applied to ensure that all bond distances fell within the normal 3.5Å range and had acceptable angles of bonding.

Computational Alanine Scans

Next, we performed a computational alanine scan to assess the contributions of charged sidechains to the stabilities of the protein complexes. To conduct this assessment, we used the alanine scan method from the computational framework AESOP (Analysis Of Electrostatic Structures of Proteins)[12-15]. This scan determined the overall contribution in terms of energy (kJ/mol) of each ionizable amino acid

when mutated to alanine individually and compared to the parent protein resulting in a change of energy (ΔΔG). Each of the energy fluctuations out of the normal range for thermal fluctuations (±2.5kJ/mol) were considered to be potentially influential residues that stabilize the protein complex.

Structural Comparisons of Electrostatic Surfaces

In order to compare electrostatic complementarity at the interface of each protein complex, we calculated electrostatic potentials for Cdk1, Cdk2, Cks1, Skp2 and $p27^{Kip1}$. The grid of electrostatic potentials calculated by the Adaptive Poisson-Boltzmann Solver (APBS)[18] were projected onto the surface of each individual protein structure within UCSF Chimera. The contacts were shown through Chimera, utilizing the find contacts and clashes feature then highlighting the selected residues to be reflected on the surface map. PBD2PQR was used to parameterize atomic radii and charges.[16,17] Surface potentials were visualized by coloring regions according to their electrostatic potential. The color scale ranges from red at -6 kT/e, the potential energy for a single proton in the corresponding region, to white at 0 kT/e and from white at 0 kT/e to blue at 6 kT/e. At this point, the complexes were then separated and displayed in the open book conformation to qualitatively assess the possible electrostatic complementarity at the contacting surfaces.

Molecular Dynamics

Finally, molecular dynamics analysis was performed on the complex of $p27^{Kip1}$ and Cks1 using NAMD and the CHARM27 force field. The structures were initially minimized with the water molecules contained in the crystallographic structure and subsequently solvated in a cubic TIP3P water box measuring 61.57Å x 63.62Å x 53.46Å. Sodium and chloride ions were also added to the water box, bringing the ionic strength to 150 mM. Minimization of the solvated structure was performed for 25,000 steps (50 ps) before heating to 310 K over 64 ps. Next, equilibration was performed where all protein atoms were constrained at 10 kcal/mol/Å^2 initially and then relaxed to 5, 2, and 1 kcal/mol/Å^2 before removing constraints altogether for the final equilibration run. Following equilibration, the MD simulation was run with periodic boundary conditions, Langevin temperature and pressure control, and particle mesh Ewald electrostatics. Relevant parameters for the simulation included a nonbonded interaction cutoff of 12 Å and a switching distance of 10 Å. Hydrogen bonds were held constant according to the SHAKE algorithm as an integration time step of 2 fs was used. The simulation was run over a 100ns timescale benchmarked at 50ps timestamps.

RESULTS

Intermolecular Hydrogen Bonds

The intermolecular hydrogen bonds between Cks1 and the adjacent chains in each of the three complexes are displayed ***(Tables 1-3)*** with the protein, three letter amino acid code, sequence number, and atom type identified for

Donor				Distance (Å)	Acceptor			
Protein	Residue	Seq. #	Atom		Protein	Residue	Seq. #	Atom
Skp2	ARG	398	NH2	3.38	Cks1	LEU	37	O
Cks1	SER	41	OG	2.77	Skp2	ASP	319	OD2
Cks1	ARG	20	NH1	3.19	$p27^{Kip1}$	THR	187	OG1
Cks1	THR	35	OG1	2.94	Skp2	THR	400	O
$p27^{Kip1}$	LYS	190	NZ	3.08	Cks1	TYR	8	O

Table 1 *details the intermolecular hydrogen bond interactions in complex Skp2-Cks1-p27Kip1 between two amino acids (donor and acceptor) of differing proteins at the complex interface, a total of 5 hydrogen bonds.*

Donor				Distance (Å)	Acceptor			
Protein	Residue	Seq. #	Atom		Protein	Residue	Seq. #	Atom
Cdk1	HIS	205	N	2.73	Cks1	GLU	63	OE2
Cdk1	GLU	206	N	3.12	Cks1	GLU	63	OE1
Cdk1	ASN	239	N	2.78	Cks1	ASP	14	OD1

Table 2 *details the intermolecular hydrogen bond interactions in complex Cdk1-Cks1 between two amino acids (donor and acceptor) of differing proteins at the complex interface, a total of 3 hydrogen bonds.*

Donor				Distance (Å)	Acceptor			
Protein	Residue	Seq. #	Atom		Protein	Residue	Seq. #	Atom
Cdk2	GLU	208	N	3.13	Cks1	GLU	63	OE1
Cdk2	GLU	208	N	2.85	Cks1	GLU	63	OE2
Cdk2	ILE	209	N	2.92	Cks1	GLU	63	OE1
Cdk2	LYS	237	NZ	3.05	Cks1	ILE	59	O
Cdk2	LYS	237	NZ	3.55	Cks1	GLU	61	OE1
Cdk2	LYS	242	N	3.09	Cks1	ASP	14	OD2
Cdk2	TRP	243	NE1	2.78	Cks1	ASP	13	O

Table 3 *details the intermolecular hydrogen bond interactions in complex Cdk2-Cks1 between two amino acids (donor and acceptor) of differing proteins at the complex interface, a total of 7 hydrogen bonds.*

donors and acceptors as well as the distance between heavy atoms. Complex Cdk2-Cks1 includes the highest amount of hydrogen bonds of the three complexes. The majority being backbone hydrogen bonds. The same observation is found in the Cdk1-Cks1 complex in smaller quantities. The Skp2- $p27^{Kip1}$-Cks1 complex has the most variation between side chain and backbone hydrogen bonds.

Computational Alanine Scans

The ΔΔG values (kJ/mol) for each ionizable amino acid when mutated to alanine, out of the range of thermal fluctuations (±2.5kJ/mol), is listed in ***Table 4*** respective to each protein, one letter amino acid code, sequence number and mutation to alanine. A negative ΔΔG value indicates a gain-of-binding mutation while a positive ΔΔG value corresponds to a loss-of-binding mutation relative to the parent sequence. There were 13 total residues that when mutated were out of the standard range of thermal fluctuations in the Cks1-Skp2- $p27^{Kip1}$ complex, split evenly between Skp2 and Cks1 with one mutation on $p27^{Kip1}$. All of the ΔΔG values for residues on Skp2 were positive while Cks1 had equal amounts positive and negative and the one value for p27Kip1 was positive. A majority, 11 of the 14 mutations recorded in the Cdk1-Cks1 complex were on the Cdk1 chain and had negative ΔΔG values. Three residues from Cks1 were recorded, one with a high negative ΔΔG value and the other 2 were positive. The Cdk2-Cks1 complex had two residues, LYS 237 and ARG 217 that displayed ΔΔG values out of the normal range and were both positive.

Cks1-Skp2- $p27^{Kip1}$			Cdk1-Cks1			Cdk2-Cks1		
Protein	Mutation	ΔΔG	Protein	Mutation	ΔΔG	Protein	Mutation	ΔΔG
Skp2	R164A	2.80	Cdk1	E232A	-7.02	Cdk1	K237A	3.65
Skp2	R344A	3.81	Cdk1	E209A	-5.67	Cdk1	R217A	3.81
Skp2	R294A	5.18	Cdk1	E163A	-5.23			
Skp2	R167A	5.40	Cdk1	D207A	-4.89			
Skp2	R398A	5.50	Cdk1	E173A	-4.80			
Skp2	D347A	5.97	Cdk1	D236A	-4.69			
Cks1	K34A	-3.15	Cdk1	D211A	-3.71			
Cks1	E40A	-3.02	Cdk1	K266A	2.62			
Cks1	E16A	-2.62	Cdk1	R218A	3.90			
Cks1	D10A	3.27	Cdk1	K243A	4.61			
Cks1	R70A	4.69	Cdk1	K238A	5.47			
Cks1	R44A	4.94	Cks1	E61A	-11.18			
$p27^{Kip1}$	E185A	4.78	Cks1	D14A	2.65			
			Cks1	R70A	4.89			

Table 4 *displays the results from the AESOP alanine scan for each complex respective to the protein, initial one letter amino acid code, sequence number, mutation to alanine and the resulting ΔΔG (kJ/mol).*

Electrostatic Surface Potentials

The electrostatic surface potentials produced by APBS are juxtaposed to the corresponding contact region, both displayed ***Figures 1-3*** in the open book conformation. The Skp2-p27^{Kip1}-Cks1 complex displays marginal, dispersed electrostatic complementarity between Skp2 and Cks1 at the contact region. In the Cdk1-Cks1 complex, there is a negative charge contact region on Cks1 that corresponds to a positively charged area on Cdk1. The Cdk2-Cks1 complex includes a negative charged region on Cks1 that appears to bind directly to a positive charge site on Cdk2.

Molecular Dynamics

The heat maps for the occupancy, or percentage of occurrence over the course of the simulation trajectory, of the interactions between Cks1 and p27^{Kip1} s are shown in ***Figure 4*** indicated by a color scale from 0.0 (0%) to 1.0 (100%) from blue to red, respectively. Multiple key residues with high rates of interaction occurrence throughout the molecular dynamics trajectory are: ARG 20, ARG 44, GLN 49, GLN 50 and SER 51 on protein Cks1. The corresponding residues and atoms on p27^{Kip1} involved in those interactions can be a target for further

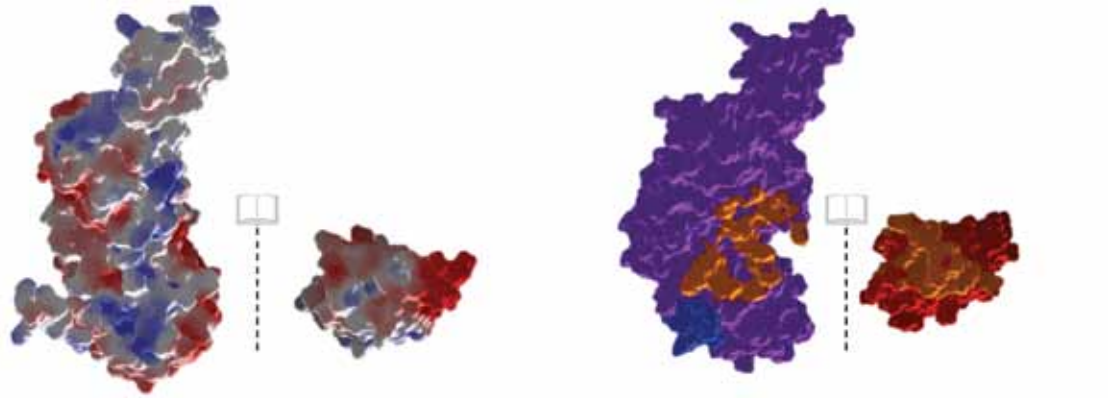

Figure 1 *displays the electrostatic projection of proteins Skp2-p27^{Kip1}-Cks1 by the range of -6kT/e to +6kT/e colored red to blue respectively with white indicating no charge. Compared to the colored surfaces distinguishing separate chains, with contacts highlighted in orange and protein Skp2 colored purple, p27^{Kip1} colored blue and Cks1 colored red.*

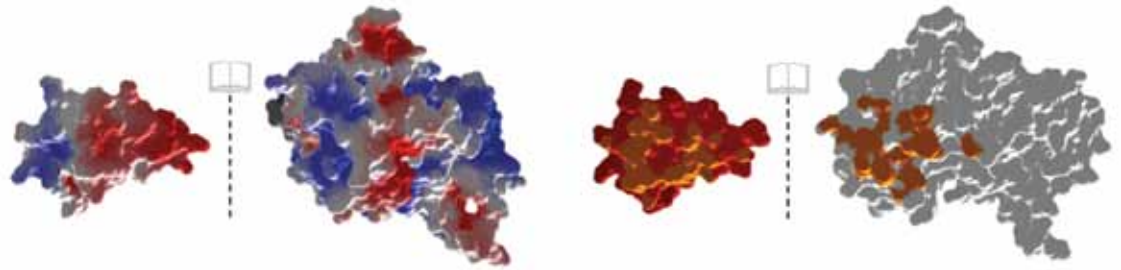

Figure 2 *displays the electrostatic projection of proteins Cdk1-Cks1 by the range of -6kT/e to +6kT/e colored red to blue respectively with white indicating no charge. Compared to the colored surfaces distinguishing separate chains, with contacts highlighted in orange and protein Cdk1 colored white and Cks1 colored red.*

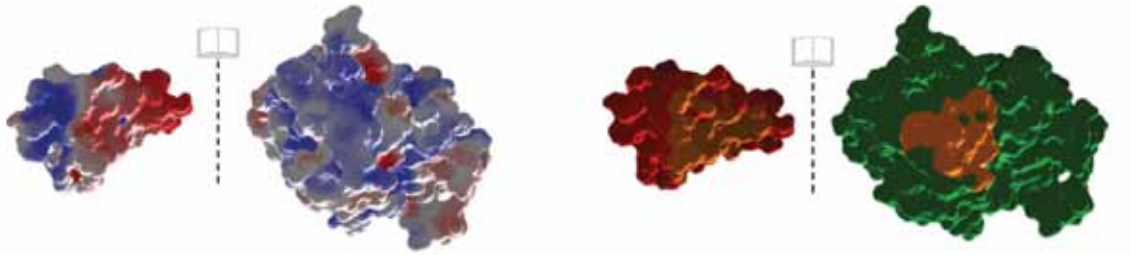

Figure 3 *displays the electrostatic projection of proteins Cdk2-Cks1 by the range of -6 kT/e to +6kT/e colored red to blue respectively with white indicating no charge. Compared to the colored surfaces distinguishing separate chains, with contacts highlighted in orange and protein Cdk2 colored green and Cks 1 colored red.*

investigation of creation of a disruptive biotherapeutic. Additionally, the heat map for the occupancy of hydrogen bonds confirms the importance of residues: ARG 20, ARG 44 and SER51 in complex stability.

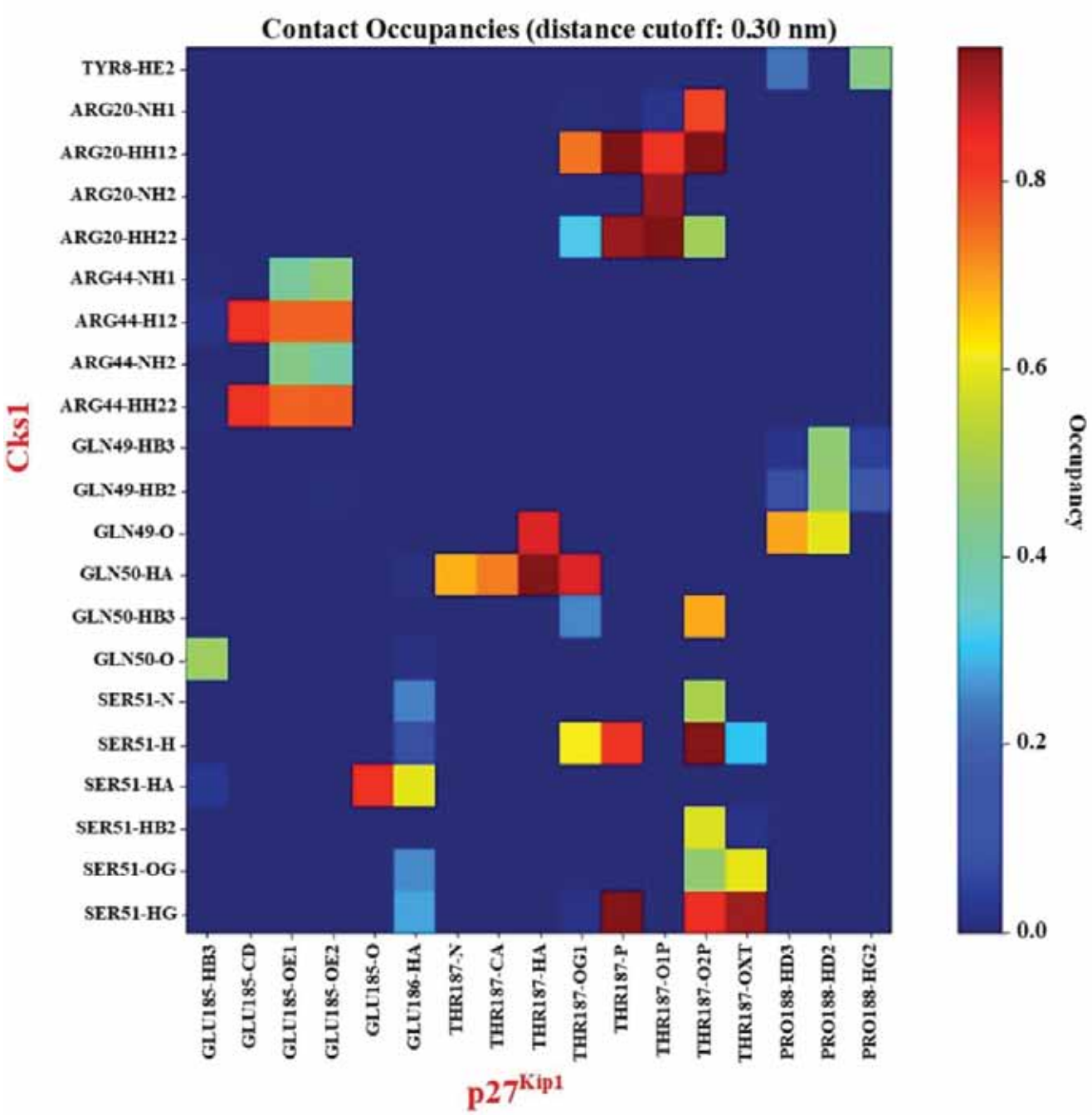

Figure 4 *displays the occupancy of interactions throughout the trajectory of the molecular dynamics simulation. Interaction sited are labeled according to the three letter amino acids code, sequence number and atom identifier with protein Cks1 on the left, vertically aligned and protein p27^{kp1} labeled on the bottom, horizontally*

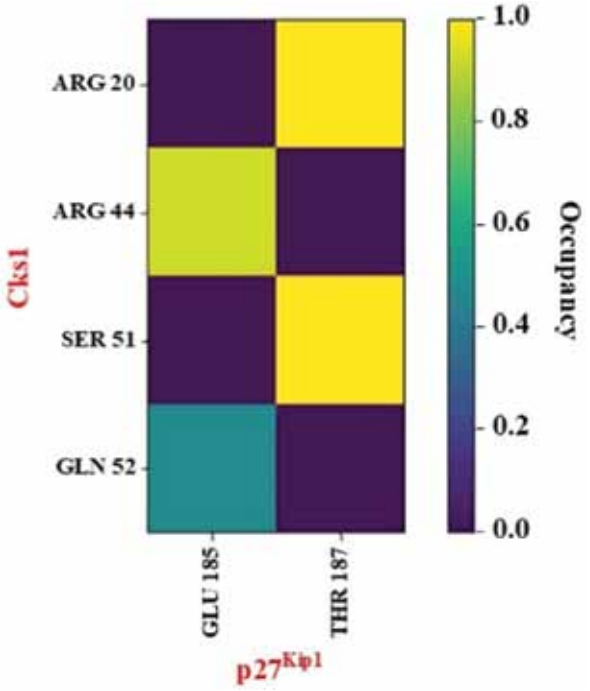

Figure 5 *diplays the occupancy of hydrogen bonds throughout the trajectory of the molecular dynamics simulation. Interaction sites are labeled according to the three letter amino acids code, sequence number and atom identifier with protein Cks1 on the left, vertically aligned and protein p27^{kp1} labeled on the bottom, horizontally.*

DISCUSSION

Intermolecular Hydrogen Bonds

Based on the hydrogen bond tables for each respective complex, all of the bonds are within the typical 3.5 Å range suggesting that these interactions are strong and contribute to the stability of the complex. There is variety between the complexes with distribution of backbone and side chain hydrogen bonds. The Cks1-Cdk1 complex having all backbone hydrogen bonds and Cks1-Cdk2 having the highest amount of total bonds in addition to the majority being to the backbone. The Skp2- p27^{Kip1}-Cks1 complex had the most diversity of types of hydrogen bonds between side chains and the backbone. Overall, with the hydrogen bonds of each system characterized by the optimal distance, angle and distribution of backbone and side chain bonds the stability of each interaction region may be difficult to disrupt.

Electrostatic Surface Potential

In Skp2-p27^{Kip1}-Cks1, translating the region of contact to the APBS electrostatic surface map shows there is a small amount of scattered electrostatic complementarity. However, there appears to be no condensed, direct complementarity at the interface suggesting that charged interactions may not play a strong role in complex stability. In Cks1-Cdk1, there potentially is direct charge complementarity at the binding interface. A small pocket of negative charge on Cks1 appears to correspond to a region of positive charge at the contact region on Cdk1 leading to suggest that these charged interactions assist in structural stability. Finally, in Cks1-Cdk2 there is no apparent direct electrostatic complementarity. The contact region on Cks1 has a negative charge and Cdk2 has an accompanying weak, positive region at the contact zone offering some reliance of the system of electrostatics for stability.

Computational Alanine Scans

Observing a direct complementarity of mutations across the complex lends to a strong interaction that can add to the stability of the complex. In Skp2- p27^{Kip1}-Cks1 there are a majority of positive, loss-of-binding mutations which happen to be in close physical proximity to each other, verified manually in Chimera. However, while there are several gain-of-binding mutations none occur in the same region as the loss-of-binding mutations. Then for Cks1-Cdk1 there is a majority of gain-of-binding mutations which are close in physical proximity. However, again there is not direct complementarity shown through the mutations and when verified in Chimera. Finally, in Cks1-Cdk2 only two ionizable amino acids are outside the effects of thermal fluctuations indicating that electrostatics may not play an important role in the complex stability.

Molecular Dynamics

The heat maps composed of the occupancies of interactions produced by molecular dynamics offers a vast amount of information regarding potential areas of targeted therapeutics. Refining down to the key interactions with high occupancies, a potential targeted attribute profile can be created to mimic these characteristics. In particular, pTHR (phosphorylated threonine) 187 on p27^{Kip1} is involved in multiple high occupancy interactions. Thus, to inhibit interactions between p27^{Kip1} and Cks1, one could attempt to prevent such interactions. Additionally, GLU 185 on p27^{Kip1} offers another source for interruption due to the large amount of hydrogen bonds between Arginine 44 on Cks1. Varying emphasis between these residues

and others at the binding pocket can lend to potential therapeutics that bind competitively to $p27^{Kip1}$ disrupting the dysfunctional cycle in cancer cells.

CONCLUSION AND PERSPECTIVE

Through the quantitative results of the hydrogen bond analysis, there are significant regions of side chain and backbone bonds stabilizing Cks1 to adjacent proteins in each of the three complexes. Additionally, through the qualitative assessment of comparing electrostatic surface potentials to the contact region and quantitative results from AESOP, charged interactions at the interface were most prevalent between the Cks1-Skp2 and Cks1-Cdk1 complexes. Through the computational evaluation of electrostatic relevance and hydrogen bonding to the stability of the three complexes, the broad contact regions between Cks1 and Skp2, CDK1, CDK2 had potential, but were not prime targets for disruption. The large binding interfaces utilized strong hydrogen bonding and electrostatic complementarity to stabilize the complex which would potentially be difficult to disrupt. However, due to the relatively small and condensed binding region between phosphorylated $p27^{Kip1}$ and Cks1, additional categorization and ranking of all possible methods of interaction is an area of future research opportunity. This led to the fine-grain analysis performed by molecular dynamics of the Cks1-$p27^{Kip1}$ system. The study revealed key interactions that occur with high frequency, notably the hydrogen bonds and charged interactions involving pTHR 187 and GLU 185 on $p27^{Kip1}$ which target SER 51, ARG 20, GLN 49 and GLN 50 on Cks1. These interactions are prime targets for developing new inhibitors for interactions between $p27^{Kip1}$ and Cks1 which can lead to new cancer therapies that restore cell cycle regulation.

ACKNOWLEDGEMENTS

I would like to sincerely thank Dr. Dimitrios Morikis and graduate student Reed Harrison from the Department of Bioengineering, as well as Dr. Jefferson Perry from the Department of Biochemistry, for suggesting this project and for the continual guidance throughout the research. I would like to also thank the members of the BioMoDeL team for additional assistance and support with the project.

REFERENCES

1. Lin HK, Chen Z, Wang G, Nardella C, Lee SW, Chan CH, Chan CH, Yang WL, Wang J, Egia A, Nakayama KI, Cordon-Cardo C, Teruya-Feldstein J, Pandolfi PP (March 2010). "Skp2 targeting suppresses tumorigenesis by Arf-p53-independent cellular senescence". Nature. 464 (7287): 374–9. doi:10.1038/nature08815. PMC 2928066 Freely accessible. PMID 20237562. Lay summary – ScienceDaily.

2. Chan CH, Lee SW, Wang J, Lin HK (2010). "Regulation of Skp2 expression and activity and its role in cancer progression". TheScientificWorldJournal. 10: 1001–15. doi:10.1100/tsw.2010.89. PMID 20526532.

3. Viglietto G, Motti ML, Bruni P, Melillo RM, D'Alessio A, Califano D, Vinci F, Chiappetta G, Tsichlis P, Bellacosa A, Fusco A, Santoro M (October 2002). "Cytoplasmic relocalization and inhibition of the cyclin-dependent kinase inhibitor p27(Kip1) by PKB/Akt-mediated phosphorylation in breast cancer". Nature Medicine. 8 (10): 1136–44. doi:10.1038/nm762. PMID 12244303.

4. Ganoth D, Bornstein G, Ko TK, Larsen B, Tyers M, Pagano M, Hershko A (March 2001). "The cell-cycle regulatory protein Cks1 is required for SCF(Skp2)-mediated ubiquitinylation of p27". Nature Cell Biology. 3 (3): 321–4. doi:10.1038/35060126. PMID 11231585.

5. Sitry D, Seeliger MA, Ko TK, Ganoth D, Breward SE, Itzhaki LS, Pagano M, Hershko A (November 2002). "Three different binding sites of Cks1 are required for p27-ubiquitin ligation". The Journal of Biological Chemistry. 277 (44): 42233–40. doi:10.1074/jbc.M205254200. PMID 12140288.

6. Murray AW (January 2004). "Recycling the cell cycle: cyclins revisited". Cell. 116 (2): 221–34. doi:10.1016/S0092-8674(03)01080-8. PMID 14744433.

7. Hao, B., Zheng, N., Schulman, B. A., Wu, G., Miller, J. J., Pagano, M., & Pavletich, N. P. (2005, October 07). Structural basis of the Cks1-dependent recognition of p27(Kip1) by the SCF(Skp2) ubiquitin ligase. Retrieved March 27, 2018, from http://www.ncbi.nlm.nih.gov/pubmed/?term=16209941

8. Brown, N. R., Korolchuk, S., Martin, M. P., Stanley, W. A., Moukhametzianov, R., Noble, M. E., & Endicott, J. A. (2015, April 13). CDK1 structures reveal conserved and unique features of the essential cell cycle CDK. Retrieved March 27, 2018, from http://www.ncbi.nlm.nih.gov/pubmed/?term=25864384

9. Bourne, Y., Watson, M. H., Hickey, M. J., Holmes, W., Rocque, W., Reed, S. I., & Tainer, J. A. (1996, March 22). Crystal structure and mutational analysis of the human CDK2 kinase complex with cell cycle-regulatory protein CksHs1. Cell 84:863-874

10. Mills, J E, and P M Dean. "Three-Dimensional Hydrogen-Bond Geometry and Probability Information from a Crystal Survey." Journal of Computer-Aided Molecular Design., U.S. National Library of Medicine, Dec. 1996, www.ncbi.nlm.nih.gov/pubmed/9007693.

11. Pettersen, E. F. et al. UCSF Chimera--a visualization system for exploratory research and analysis. Journal of Computational Chemistry 25, 1605–1612 (2004).

12. Harrison RES, Mohan RR, Gorham RD Jr, Kieslich CA, Morikis D (2017) AESOP: A python library for investigating electrostatics in protein interactions, Biophysical Journal 112:1761-1766.

13. Gorham, R. D. et al. An evaluation of Poisson–Boltzmann electrostatic free energy calculations through comparison with experimental mutagenesis data. Biopolymers 95, 746–754(2011).

14. Kieslich, C. A., Gorham Jr., R. D. & Morikis, D. Is the rigid-body assumption reasonable?: Insights into the effects of dynamics on the electrostatic analysis of barnase–barstar. Journal of Non-Crystalline Solids 357, 707–716 (2011).

15. Gorham, R. D., Kieslich, C. A. & Morikis, D. Electrostatic Clustering and Free Energy Calculations Provide a Foundation for Protein Design and Optimization. Annals of Biomedical Engineering 39, 1252–1263(2011).

16. Dolinsky, T. J., J. E. Nielsen, ., N. A. Baker. 2004. PDB2PQR: an automated pipeline for the setup of Poisson-Boltzmann electrostatics calculations. Nucleic Acids Research 32:W665–W667.

17. Dolinsky, T. J., P. Czodrowski, ., N. A. Baker. 2007. PDB2PQR: expanding and upgrading automated preparation of biomolecular structures for molecular simulations. Nucleic Acids Res. 35:W522-W525

18. Baker, N. A., D. Sept, Simpson, Joseph, J. A. McCammon. 2001. Electrostatics of nanosystems: application to microtubules and the ribosome. Proceedings of the National Academy of Sciences of USA. 98:10037–10041.